

# Invasion speeds for structured populations in fluctuating environments

Sebastian J. Schreiber

Maureen E. Ryan

*Department of Evolution and Ecology and the Center for Population Biology  
University of California, Davis, California 95616*

## ABSTRACT

1 We live in a time where climate models predict future increases in environmen-  
2 tal variability and biological invasions are becoming increasingly frequent. A key  
3 to developing effective responses to biological invasions in increasingly variable en-  
4 vironments will be estimates of their rates of spatial spread and the associated un-  
5 certainty of these estimates. Using stochastic, stage-structured, integro-difference  
6 equation models, we show analytically that invasion speeds are asymptotically nor-  
7 mally distributed with a variance that decreases in time. We apply our methods to  
8 a simple juvenile-adult model with stochastic variation in reproduction and an il-  
9 lustrative example with published data for the perennial herb, *Calathea ovandensis*.  
10 These examples buttressed by additional analysis reveal that increased variability  
11 in vital rates simultaneously slow down invasions yet generate greater uncertainty  
12 about rates of spatial spread. Moreover, while temporal autocorrelations in vital  
13 rates inflate variability in invasion speeds, the effect of these autocorrelations on the  
14 average invasion speed can be positive or negative depending on life history traits  
15 and how well vital rates “remember” the past.

**Word count:** 4,649 without Appendix; 4,807 with Appendix

**Figures:** 4 **Tables:** 0 **References:** 50

## Introduction

16

17 Anthropogenic forces are changing the temporal distribution of environmental fluctuations  
18 and accelerating the rate at which species are being introduced into non-native habitat. Gen-  
19 eral circulation models predict increased variability in temperatures and precipitation and these  
20 changes are likely to increase variability in vital rates of many species (Easterling et al. 2000;  
21 Tebaldi et al. 2006; Boyce et al. 2006). Alternatively, human activities such as agriculture,  
22 recreation, and transportation are spreading species beyond their natural dispersal barriers (El-  
23 ton 1958; Kolar and Lodge 2001). While most of these accidental or intentional introductions  
24 fail, the successful invaders can have devastating impacts on human health and native biodiver-  
25 sity (Kolar and Lodge 2001). To manage these impacts, it is essential to understand the rate  
26 of range expansion—the invasion speed—of these invaders. Here, we bring together the theory of  
27 stochastic demography and invasion speeds to provide a general framework to estimate invasion  
28 speeds for structured populations in a variable environment.

29 Stochastic demography is concerned with understanding population growth and distribution  
30 when vital rates vary in time due to stochastic fluctuations in environmental variables (Boyce  
31 et al. 2006). In their simplest guise, models of stochastic demography are the form  $\mathbf{n}_{t+1} = \mathbf{A}_t \mathbf{n}_t$   
32 where  $\mathbf{n}_t$  is the vector of population abundances in the different stages at time  $t$  and  $\mathbf{A}_t$  is a  
33 projection matrix whose entries describe fluxes between stages due to combinations of growth,  
34 survivorship, and reproduction. These models play a critical role in identifying to what extent  
35 variation in vital rates alter the stochastic growth rate of a population (Tuljapurkar 1990; Tul-  
36 japurkar et al. 2003; Haridas and Tuljapurkar 2005; Morris et al. 2008). For example, Morris  
37 et al. (2008) analyzed multiyear demographic data for 36 plant and animal species and found  
38 that the stochastic growth rate of short-lived species (insects, annual plants, and algae) are  
39 more negatively affected by increased variation in vital rates than longer-lived species (peren-  
40 nial plants, birds, ungulates). Correlations between vital rates within a year or autocorrelations  
41 in vital rates in successive years can significantly effect stochastic growth rates. Analytic ap-  
42 proximations imply that negative correlations between vital rates can buffer the effects of de-  
43 mographic stochasticity and thereby increase stochastic growth rates (Tuljapurkar 1990; Boyce  
44 et al. 2006). In contrast, temporal autocorrelations can increase or decrease stochastic growth  
45 rates, and increases in these autocorrelations can have larger impacts on growth than increases  
46 in inter-annual variability of vital rates (Tuljapurkar 1990; Tuljapurkar and Haridas 2006).

47 For populations not experiencing an Allee effect, a positive growth rate at low densities is  
48 necessary for establishment and range expansion. An important class of models for predicting  
49 rates of range expansion are integro-difference equation (IDE) models (Kot et al. 1996) in which  
50 a dispersal kernel describes the likelihoods that individuals move between locations. For diffusive  
51 movement, this kernel is a Gaussian and the rate of spread equals  $2\sqrt{rD}$  where  $D$  is the diffusion  
52 rate and  $r$  is the intrinsic rate of growth of the population (Kot et al. 1996); the same rate of  
53 spread first derived by Fisher (1937) for reaction-diffusion equations. While this estimate of  
54 rate of spread has been applied to many species (Hengeveld 1994), field estimates of dispersal  
55 kernels typically are leptokurtic and not Gaussian (Kot et al. 1996) and, consequently, this  
56 earlier work may underestimate invasion speeds. Using stochastic counterparts to these IDE  
57 models, Neubert et al. (2000) showed that serially uncorrelated, stochastic fluctuations generate  
58 normally distributed invasion speeds whose variance decays to zero. Hence, invasion speeds may  
59 exhibit unpredictable transients in fluctuating environments. On the other hand, Neubert and  
60 Caswell (2000) developed methods to estimate invasion speeds for stage-structured IDE models  
61 that have been invaluable for identifying how stage-specific vital rates constrain rates of spatial  
62 spread (Caswell et al. 2003; Jacquemyn et al. 2005; Jongejans et al. 2008). However, the dual  
63 effects of demographic and temporal heterogeneity on rates of range expansion remains to be  
64 understood.

65 Here, we provide a framework for analyzing the simultaneous effects of environmental fluc-  
66 tuations and demographic structure on invasion speeds. We begin by reviewing the work of  
67 Neubert and Caswell (2000) in constant environments. We extend these models to allow for  
68 temporal variation in the projection matrices and dispersal kernels and provide a formula for  
69 asymptotic invasion speeds and normal approximations that describe the variation in these inva-  
70 sion speeds over finite time horizons. Applying these results to two examples, we illustrate how  
71 our results allow one to address questions like “how does the magnitude of variability influence  
72 asymptotic invasion speeds?” and “how do temporal autocorrelations influence the uncertainty  
73 in predicting invasion speeds?”

## 74 **Constant environments**

75 Neubert and Caswell (2000) analyzed invasion speeds for IDE models for stage-structured  
76 populations in constant environments. These models consider structured populations living on

77 a continuous one-dimensional habitat and consisting of  $m$  stages where  $n_t^i(x)$  is the density  
 78 of stage  $i$  at time  $t$  in location  $x$ . Let  $b^{ij}(n^1(x), \dots, n^m(x))$  be the contribution of stage  $j$   
 79 individuals to stage  $i$  individuals at location  $x$ . Let  $k^{ij}(x)$  be the probability density function  
 80 for the displacement  $x$  moved by an individual transitioning from stage  $j$  to  $i$ . Under these  
 81 assumptions, the dynamics of the population are given by

$$n^i(x) = \int_{-\infty}^{\infty} \sum_{j=1}^m k^{ij}(x-y) b^{ij}(n_t^1(y), \dots, n_t^m(y)) n_t^j(y) dy$$

82 To simplify the notation, let  $\mathbf{n}_t(x) = (n_t^1(x), \dots, n_t^m(x))'$  where  $'$  denotes transpose be the vector  
 83 of population abundances at time  $t$  and location  $x$ . Let  $\mathbf{B}(\mathbf{n}_t(x))$  and  $\mathbf{K}(x)$  denote the  $m \times m$   
 84 matrices with entries  $b^{ij}(\mathbf{n}_t(x))$  and  $k^{ij}(x)$ , respectively. With this notation, we get the simplified  
 85 equation

$$\mathbf{n}_{t+1}(x) = \int_{-\infty}^{\infty} [\mathbf{K}(y-x) \circ \mathbf{B}(\mathbf{n}_t(y))] \mathbf{n}_t(y) dy \quad (1)$$

86 where  $\circ$  denotes the Hadamard product i.e. component wise multiplication.

87 When the population is unstructured (i.e.  $m = 1$ ), model (1) has traveling waves-solutions  
 88 that maintain a fixed shape in space and move at a constant speed. If the growth function  $b(n)n$   
 89 increases with population density,  $b(n)$  is decreasing (i.e. no Allee effect), and the dispersal  
 90 kernel possesses a moment-generating function  $m(s) = \int_{-\infty}^{\infty} k(x)e^{-sx} dx$  for  $0 \leq s < \hat{s}$ , then the  
 91 traveling wave has an asymptotic speed

$$c^* = \min_{0 < s < \hat{s}} \frac{1}{s} \ln [b(0)m(s)]$$

92 A population initially concentrated in a finite region of space will never spread faster than  
 93  $c^*$  and asymptotically will spread at a rate of exactly  $c^*$  (Weinberger 1982). The linearization  
 94 conjecture states that the speed of invasion for a nonlinear model is governed by its linearization  
 95 at low population densities, as long as there are no Allee effects and no long-distance density  
 96 dependence. This conjecture is supported by many numerical studies.

97 Relying on the linearization conjecture, Neubert and Caswell (2000) derived a formula for  
 98 traveling wave speeds for structured populations. This derivation makes four assumptions: (1)  
 99 the matrices  $\mathbf{B}(\mathbf{n})$  are non-negative and primitive, (2)  $\mathbf{A} = \mathbf{B}(0)$  has a dominant eigenvalue  $\rho(\mathbf{A})$   
 100 that is greater than one, (3) there is negative density dependence i.e.  $\mathbf{B}(\mathbf{n}) \leq \mathbf{A}\mathbf{n}$  for all  $\mathbf{n} \geq 0$   
 101 where inequalities are taken componentwise, and (4) the kernels  $k^{ij}(x)$  have moment generating

102 functions  $m^{ij}(s)$  defined on some maximal interval  $0 \leq s < \hat{s}$ . Under these assumptions, Neubert  
 103 and Caswell (2000) showed the asymptotic wave speed is given by

$$c^* = \min_{0 < s < \hat{s}} \frac{1}{s} \log \rho(\mathbf{A} \circ \mathbf{M}(s)) \quad (2)$$

104 where  $\mathbf{M}(s)$  is the matrix of moment generating functions  $m^{ij}(s)$ .

### 105 Fluctuating environments

106 To account for temporal variation in environmental conditions and dispersal rates, we allow  
 107  $\mathbf{B}_t(\mathbf{n})$ , and  $\mathbf{K}_t(x)$  to depend on time. In which case,

$$\mathbf{n}_{t+1}(x) = \int_{-\infty}^{\infty} [\mathbf{K}_t(x-y) \circ \mathbf{B}_t(\mathbf{n}_t(y))] \mathbf{n}_t(y) dy \quad (3)$$

108 In order to make use of the linearization conjecture, we place four assumptions on (3). First,  
 109 the populations exhibit negative density dependence in which case  $\mathbf{A}_t := \mathbf{B}_t(0) \leq \mathbf{B}_t(\mathbf{n})$  for all  
 110  $\mathbf{n} \geq 0$ . Second, there exists  $n_0 > 0$  such that  $\mathbf{A}_{n_0} \dots \mathbf{A}_1$  has all positive entries with probability  
 111 one. This assumption ensures the effects of the initial distribution of the population disappear in  
 112 the limit (demographic weak ergodicity). Third, there exists a  $\hat{s} > 0$  such that the kernels  $k_t^{ij}(x)$   
 113 have moment generating functions  $m_t^{ij}(s)$  defined for  $0 \leq s < \hat{s}$ . We always choose  $\hat{s}$  to be the  
 114 maximum of these values. Without this assumption, solutions may accelerate and have no well-  
 115 defined asymptotic wave speed (Kot et al. 1996). To state the fourth assumption, let  $\mathbf{M}_t(s)$  be  
 116 the matrix with entries  $m_t^{ij}(s)$  and  $\mathbf{H}_t(s) = \mathbf{M}_t(s) \circ \mathbf{A}_t$ . We assume that the sequence of matrices,  
 117  $\mathbf{H}_0(s), \mathbf{H}_1(s), \dots$  are stationary and ergodic and  $\mathbb{E}[\max\{\ln \|\mathbf{H}_t(s)\|, 0\}] < \infty$  for all  $0 \leq s < \hat{s}$ .  
 118 This assumption encompasses many models of environmental fluctuations including periodic,  
 119 quasi-periodic, irreducible Markovian, and auto-regressive models. Under this assumption, the  
 120 random version of the Perron-Frobenius theorem (Arnold et al. 1994) implies that for any  $\mathbf{n} > 0$   
 121 and  $\mathbf{w} > 0$  (i.e. all components are non-negative and at least one is positive)

$$\lim_{t \rightarrow \infty} \frac{1}{t} \ln \langle \mathbf{H}_{t-1}(s) \dots \mathbf{H}_0(s) \mathbf{n}, \mathbf{w} \rangle = \gamma(s) \text{ with probability one} \quad (4)$$

122 where  $\gamma(s)$  is the dominant Lyapunov exponent associated with this random product of matrices  
 123 and  $\langle \cdot, \cdot \rangle$  denotes the standard Euclidean inner product. When  $s = 0$  and  $\mathbf{w} = (1, \dots, 1)'$ , this  
 124 Lyapunov exponent

$$\gamma(0) = \lim_{t \rightarrow \infty} \frac{1}{t} \ln \langle \mathbf{A}_{t-1}(s) \dots \mathbf{A}_0(s) \mathbf{n}, \mathbf{w} \rangle$$

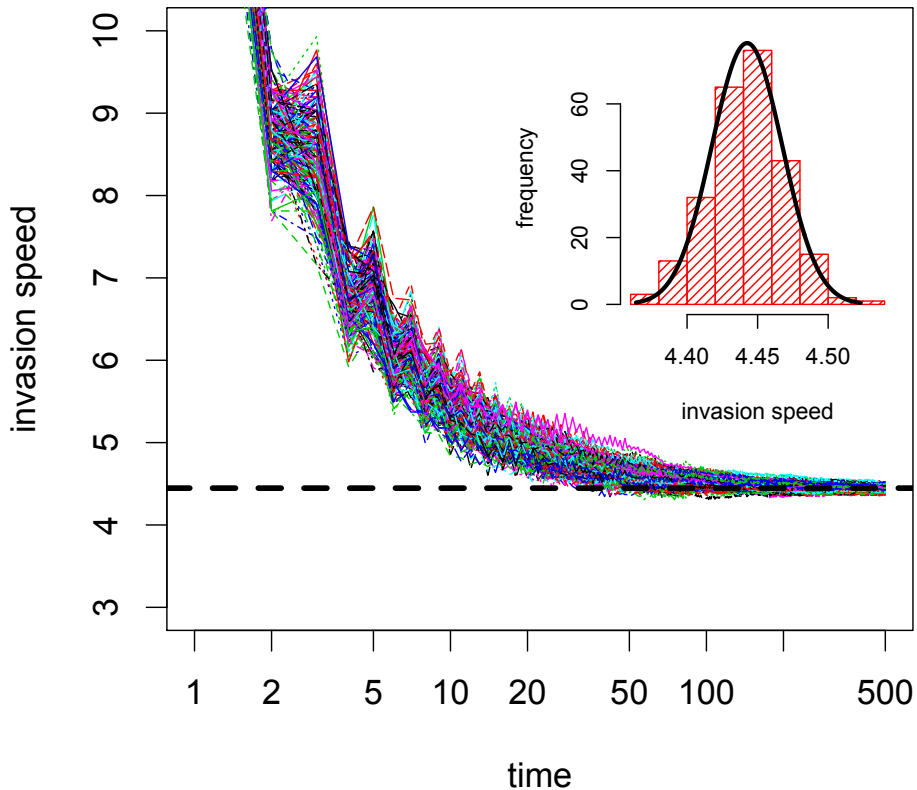


Fig. 1.— The temporal dynamics of the wave speed  $\frac{X_t - x_0}{t}$  for 250 simulations of the non-linear juvenile-adult model. The front of the wave was determined by a threshold of  $n_c = 0.001$  with equal weight on both stages i.e.  $\mathbf{w} = (1, 1)'$ . The dashed line is the predicted asymptotic wave speed in (5). In the inset, a histogram of the waves speeds at  $t = 500$  with the predicted normal approximation from the linearization. Parameter values are  $\rho = 0$ ,  $\mu = \ln 40$ ,  $\sigma = 0.5$ ,  $a = 1$ ,  $s_J = 0.3$ , and  $s_A = 0.4$ .

125 describes the growth rate of the total population size when rare (Tuljapurkar 1990). Since  
 126 an invasion can only proceed if the population has the capacity to exhibit growth, our final  
 127 assumption is that  $\gamma(0) > 0$ .

128 When demographic or dispersal rates vary in time, the rate of spatial spread will vary in  
 129 time. To quantify this rate of spread, assume there is a weighting  $\mathbf{w} > 0$  of the different stages  
 130 and a weighted population abundance,  $n_c > 0$ , above which the population is observable. At  
 131 time  $t$ , let  $X_t$  denote the location furthest from the invasion's origin at which  $\langle \mathbf{n}_t(s), \mathbf{w} \rangle \geq n_c$ .

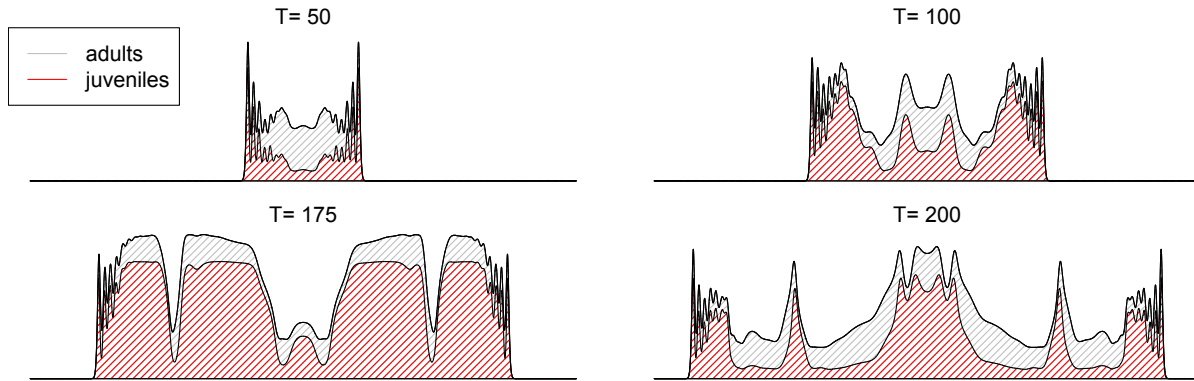


Fig. 2.— Spatio-temporal dynamics of range expansion for the juvenile-adult model. Spatial distribution and abundance of juveniles (in shaded red) and adults (in shaded grey) plotted at the indicated times. Parameters ( $\rho = 0$ ,  $\mu = \ln 40$ ,  $\sigma = 0.1$ ,  $a = 1$ ,  $s_J = 0.3$ , and  $s_A = 0.4$ ) are such that local dynamics are chaotic.

132 The average speed  $C_t$  of the invasion by time  $t$  is given by  $\frac{X_t - x_0}{t}$  where  $x_0$  is the introduction  
 133 site. In Appendix A we show that with probability one,  $\frac{X_t - x_0}{t}$  is asymptotically bounded above  
 134 by

$$c^* = \min_{0 \leq s < \hat{s}} \frac{\gamma(s)}{s} \quad (5)$$

135 whenever  $\mathbf{n}_0(x)$  has compact support. The linearization conjecture and our numerical results  
 136 (Fig. 1) suggest that  $c^*$  is not only an upper bound but in fact equals the asymptotic wave speed  
 137 with probability one. In the special case of periodic environmental fluctuations (i.e. there exists  
 138 a natural number  $p$  such that  $\mathbf{A}_{t+p} = \mathbf{A}_t$  and  $\mathbf{K}_{t+p}(x) = \mathbf{K}_t(x)$  for all  $t$  and  $x$ ), the asymptotic  
 139 invasion speed is given by

$$c^* = \min_{s > 0} \frac{1}{sp} \ln \rho \left( \prod_{t=1}^p \mathbf{A}_t \mathbf{M}_t(s) \right)$$

140 where  $\rho$  denotes the dominant eigenvalue of a matrix.

141 Under the additional assumption that matrices  $\mathbf{H}_t(s)$  are rapidly mixing (see, e.g., Heyde  
 142 and Cohen (1985)), Appendix B shows that there exists  $\sigma > 0$  such that the average speeds  $\frac{X_t - x_0}{t}$   
 143 are asymptotically normal with mean  $c^*$  and standard deviation  $\sigma/(s^* \sqrt{t})$ . This approximation  
 144 is consistent with numerical simulations of the nonlinear models (inset of Fig. 1). In the special  
 145 case of an unstructured population  $m = 1$ , this result extends Neubert et al. (2000)'s work on  
 146 uncorrelated environments to correlated environments. In this case, the central limit theorem

147 for stationary sequences of random variables (Durrett 1996) implies

$$\sigma^2 = \text{Var}[\ln \mathbf{H}_1(s^*)] + 2 \sum_{i=2}^{\infty} \text{Cov}[\ln \mathbf{H}_1(s^*), \ln \mathbf{H}_i(s^*)] \quad (6)$$

148 where  $s^*$  is such that  $c^* = \gamma(s^*)/s^*$ . For unstructured populations, equation (6) implies that pos-  
 149 itive temporal autocorrelations increase the variability in asymptotic wave speeds while negative  
 150 autocorrelations reduce this variability. In contrast, as  $\gamma(s) = \mathbb{E}[\ln H_1(s)]$ , temporal autocorre-  
 151 lations have no effect on the mean  $c^*$  invasion speed for unstructured populations.

152 To illustrate the applicability of our results to structured populations, we consider two  
 153 examples. The first example is a simple juvenile-adult structure model with continuous variation  
 154 in fecundity rates. We use this example to illustrate the accuracy of the linear approximation, the  
 155 dynamics of spatial spread, and the effects of noise amplitude and color on invasion speeds and  
 156 stochastic growth. In the second example, we analyze the effects of environmental stochasticity  
 157 on invasion speeds for an herbaceous perennial herb, *Calathea ovandensis* (*Marantaceae*). This  
 158 example was studied for constant environments by Neubert and Caswell (2000). Here, we  
 159 illustrate the effects of the frequency of poor environmental conditions and temporal correlations  
 160 on invasion speeds and their uncertainty using empirical data.

161 **Example: Fluctuating fecundities.** We consider a population with two stages, juvenile  
 162 and adult, in which dispersal occurs following reproduction. We assume that the per-capita  
 163 fecundity  $f_t \exp(-a n_t^2)$  is density-dependent where  $n_t^2$  is the adult density at time  $t$ ,  $f_t$  is the  
 164 maximal fecundity at time  $t$ , and  $a > 0$  measures the intensity of intraspecific competition. Let  
 165  $s_J$  denote the fraction of juveniles surviving to adulthood, and  $s_A$  denote the fraction of adults  
 166 that survive to the next year. Under these assumptions,

$$\mathbf{B}_t(\mathbf{n}) = \begin{pmatrix} 0 & f_t \exp(-a n_t^2) \\ s_J & s_A \end{pmatrix}$$

167 We assume that  $\log f_t$  are normally distributed with mean  $\mu$ , variance  $\sigma^2$ , and temporal corre-  
 168 lation  $\rho$  between  $\log f_t$  and  $\log f_{t+1}$ . Dispersal follows birth with a Laplacian distribution with  
 169 variance  $2b^2$ . Hence, the moment generating matrix for this model is

$$M(s) = \begin{pmatrix} 1 & \frac{1}{1-(bs)^2} \\ 1 & 1 \end{pmatrix}$$



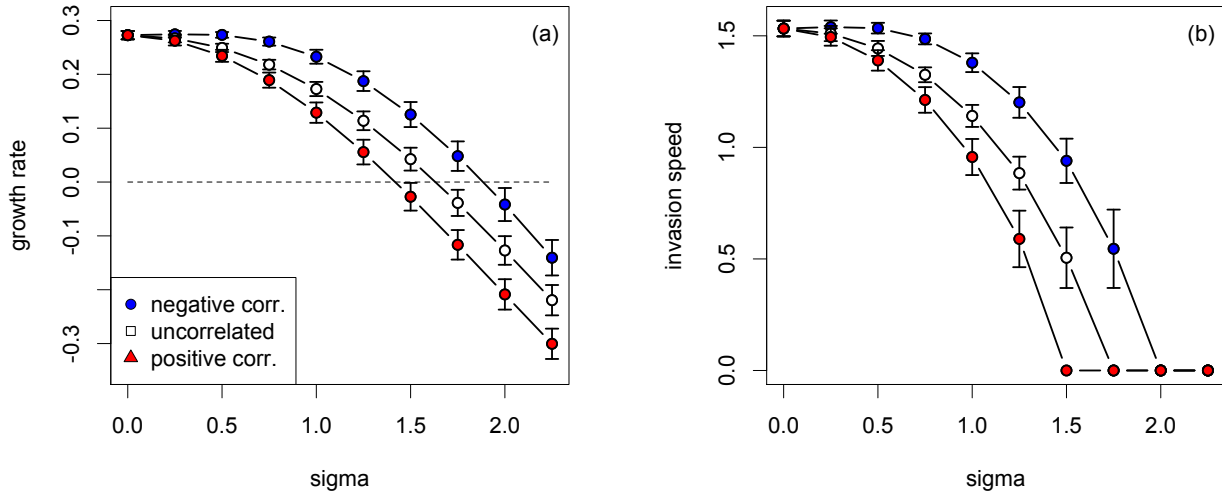


Fig. 3.— The stochastic growth rate  $\gamma$  and invasion speed  $c^*$  plotted as a function of the standard deviation of the log fecundity  $\log f_t$ . Length of error bars correspond to the standard deviation in the growth rate after 400 generations. The blue, white, and red curves correspond to temporal correlations of  $\rho = -0.5, 0$  and  $0.5$ . Parameters are such that  $\mathbb{E}[f_t] = 4$ ,  $s_J = 0.3$ , and  $s_A = 0.4$ . Simulations for estimates ran for 10,000 generations.

170 which is defined for  $0 \leq s \leq \hat{s} = 1/b$ . When adults are highly fecund, the interaction between  
 171 locally unstable population dynamics and environmental stochasticity can generate complex  
 172 spatial-temporal patterns of range expansion (Fig. 2). None the less, simulations of the full  
 173 nonlinear mode suggest that linearization conjecture holds (Fig. 1).

174 To understand the effects of temporal variation and correlations on wave speeds and popula-  
 175 tion growth, we computed  $\gamma(0)$ ,  $c^*$ , and standard deviations of both of these quantities for a range  
 176 of  $\mu$  and  $\sigma^2$  values. In all of these simulations, we held the mean fecundity  $\mathbb{E}[f_t] = \exp(\mu - \sigma^2/2)$   
 177 constant at 4. The simulations show that the population growth rate  $\gamma(0)$  and the asymp-  
 178 totic wave speed decreases both with increasing temporal variation and increasing temporal  
 179 autocorrelations (Fig. 3). In particular, when this variation is too high, the population has a  
 180 negative stochastic growth rate and does not propagate. Autocorrelations have little effect on  
 181 the variability of the stochastic growth rates, but variation in invasion speeds increases with  
 182 autocorrelations.

183 **Example: *Calathea ovandensis*.** *Calathea ovandensis* is an understory monocot, found  
 184 in neotropical lowland rain forests (Horvitz and Schemske 1995). Deciduous during the dry  
 185 season, *C. ovandensis* plants reinitiate growth from rhizomes during the rainy season and bear  
 186 fruit capsules, which dehisce to expose large seeds that fall to the forest floor (Horvitz and  
 187 Beattie 1980). Seeds are myrmecochorous (adapted for ant dispersal), bearing oily white arils  
 188 (eliasomes) that are considered arthropod prey mimics (Carroll and Janzen 1973). Ponerine  
 189 ants carry seeds to their nests like prey, remove and consume the arils, and bury seeds in  
 190 nitrogen-rich garbage piles of dead insect prey near the nest entrance (Horvitz and Beattie  
 191 1980; Horvitz and Schemske 1995).

192 At Horvitz and Schemske’s study site in southern Mexico, four ant species act as dispersal  
 193 agents: *Pachycondyla apicalis*, *P. harpax*, *Solenopsis geminata*, and *Wasmannia auropunctata*  
 194 (Horvitz and Schemske 1995). *Calathea ovandensis* do not propagate vegetatively, and empirical  
 195 distributions of seedlings are well matched to ant dispersal distances (Horvitz and Schemske  
 196 1986). Horvitz and Schemske (1995) measured demographic rates, constructing 16 projection  
 197 matrices for four sites over four years, and found that *C. ovandensis*’ highest population growth  
 198 rates occurred during el Niño years and in plots affected by treefall gaps (Horvitz and Schemske  
 199 1995; C. Horvitz and Caswell 1997).

200 We selected 3 stage-structured matrices that represent 1) the highest population growth,  
 201 observed during an el Niño year ( $\lambda = 1.2477$ ; plot 2, 1982-83; also used in Neubert and Caswell  
 202 (2000)), 2) lowest (negative) growth in the same plot ( $\lambda = 0.9051$ ; plot 2; 1984-85), and 3) the  
 203 worst year-plot combination overall ( $\lambda = 0.7356$ ; plot 3, 1984-85). Individuals are classified as  
 204 seeds, seedlings, juveniles, pre-reproductives, and small, medium, large and extra-large adult  
 205 plants (for life cycle graph, see Neubert and Caswell (2000)). Seed dispersal involves transitions  
 206 from most stages. We follow Neubert and Caswell (2000) in assuming a Laplace distribution  
 207 of dispersal distances of four ant species and weighting dispersal by the relative abundance of  
 208 each species (Horvitz and Schemske 1995; Neubert and Caswell 2000). This treatment assumes  
 209 that seed fates are independent of dispersal agent (Neubert and Caswell 2000), and yields the  
 210 dispersal kernel matrix

$$K(x - y) = \sum_{i=1}^4 p_i K_i(x - y)$$

211 where  $p_i$  are the proportion of seeds dispersed by each ant species, and  $K_i(x - y)$  is a matrix  
 212 whose first row contains Laplace dispersal kernels with generating functions  $m_i(s) = 1/(1 - b_i^2 s^2)$

213 with parameter  $b_i$ , representing the mean distance a seed is moved by a particular ant species  
 214 as reported by Horvitz and Schemske (1986), and Delta functions for the remaining entries  
 215 (Neubert and Caswell 2000). The moment-generating function matrix is

$$M(s) = \sum_{i=1}^4 p_i M_i(s)$$

216 where  $M_i(s)$  is the moment generating function for  $K_i(x)$ .

217 We ran two types of simulations representing (1) random fluctuations between environmen-  
 218 tal states corresponding to the highest population growth and the lowest population growth in  
 219 the same plot (i.e. randomly varying between the matrices with dominant eigenvalues  $\lambda = 1.2477$   
 220 and  $\lambda = 0.9051$ ) and (2) random fluctuations between environmental states corresponding to the  
 221 highest and lowest overall population growth across all sites (i.e.  $\lambda = 1.2477$  and  $\lambda = 0.7356$ ).  
 222 For each of these simulations, switches between “good” and “bad” years were modeled by a  
 223 Markov chain in which the probability of transition from a bad year to a good year is  $q$  and the  
 224 probability of transition from a good year to a bad year is  $p$ . For this model of the environmen-  
 225 tal dynamics, the long-term frequency of good years is  $\frac{q}{q+p}$  and the temporal autocorrelation  
 226 between environmental states is  $1 - q - p$ . For both scenarios, simulations were run for all  
 227 combinations of  $p$  and  $q$  values to determine the combined effects of frequency of good years  
 228 and temporal correlations on stochastic growth and invasion speed.

229 Both the stochastic growth rate and invasion speed were strongly correlated with the overall  
 230 frequency of good years, while correlations between environmental states had a relatively small  
 231 effect on asymptotic growth rates and invasion speeds (Fig. 4). However, positive correlations  
 232 between environmental states did increase growth rates and invasion speeds, while negative  
 233 correlations reduced both (left and middle column of Fig. 4). For growth rates, the effect of  
 234 correlations was greatest when the frequency of good and bad years were equal ( $q/(q+p) = 0.5$ )  
 235 (left column of Fig. 4), presumably since the largest number of combinations of  $(p, q)$  values  
 236 can generate this frequency. Environmental correlations had the greatest impact on invasion  
 237 speeds near the threshold between positive and zero growth (middle column of Fig. 4), where  
 238 invasion speeds also exhibited the greatest variance (right column of Fig. 4). As a result, near the  
 239 threshold in parameter values between positive and negative growth rates (and hence positive  
 240 or zero invasion speed), the magnitude and sign of correlations between environmental states  
 241 determined whether populations grew and spread or declined. For example, for scenario one

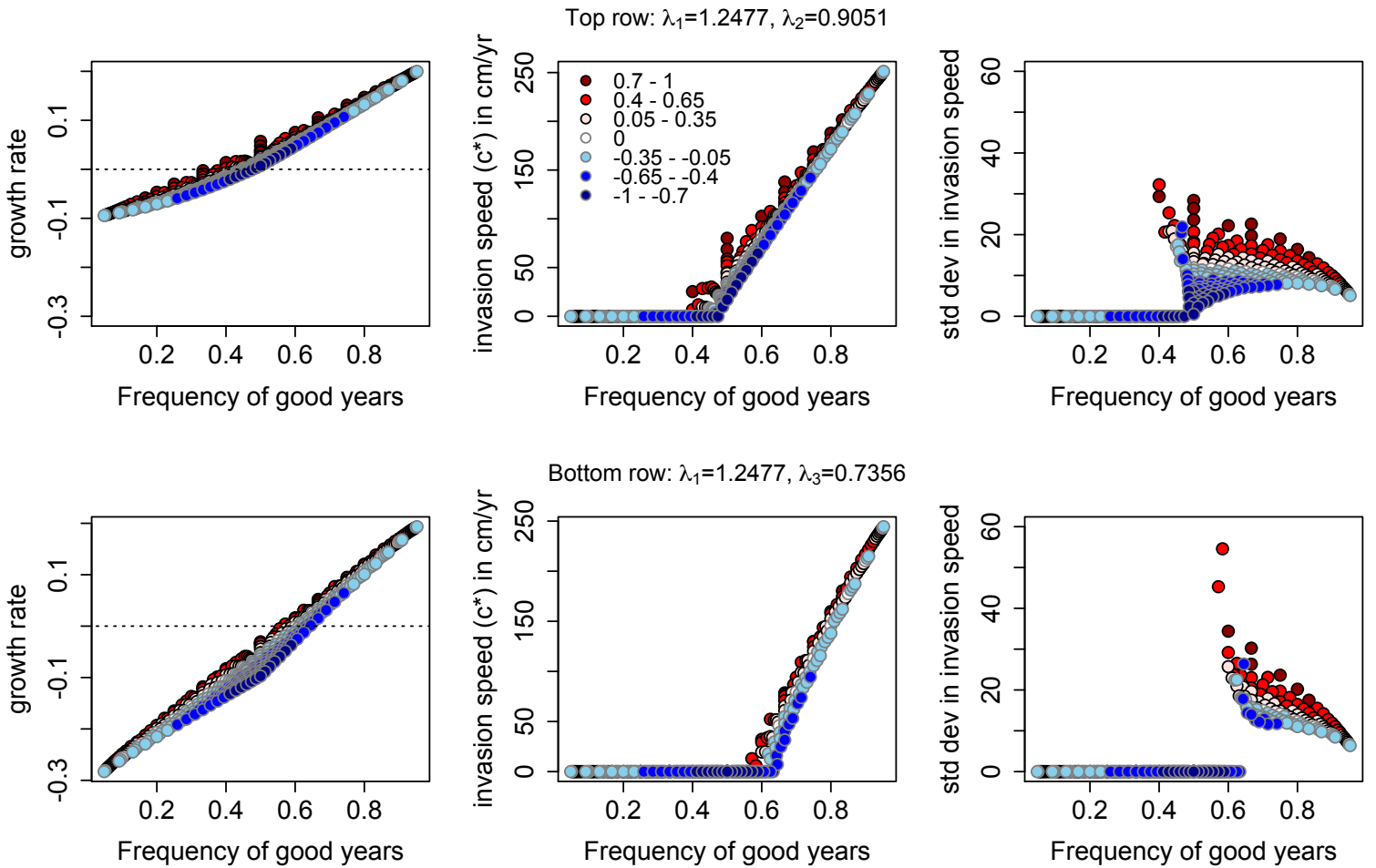


Fig. 4.— Stochastic growth rates and invasion speeds ( $c^*$ ) for *Calathea ovandensis*. Stochastic growth rates (left column), asymptotic invasion speeds (middle column), and standard deviation in invasion speeds after 400 years (right column) are plotted as a function of the frequency  $q/(q+p)$  of good years for all probabilities  $p$  and  $q$  of switching from “good” to “bad” years and vice versa. Temporal correlations associated with the different  $p, q$  combinations are plotted in color as indicated in the legend. Figures in the top row correspond to random fluctuations between environmental states corresponding to the highest population growth and the lowest population growth in the same plot (i.e.  $\lambda = 1.2477$  and  $\lambda = 0.9051$ ). Figures in the bottom row correspond to random fluctuations between environmental states corresponding to the highest and lowest overall population growth across all sites (i.e.  $\lambda = 1.2477$  and  $\lambda = 0.7356$ ). Simulations ran for 100,000 generations.

242 (top row of Fig. 4), strong positive correlations allowed the population to grow when only 35%  
 243 of years were good, while strong negative correlations generated negative growth rates under  
 244 the same scenario even at nearly even proportions of good and bad years.

245 Like growth rates and invasion speed, variance in invasion speed was also strongly affected  
246 by both environmental correlation and the frequency of good years (right column of Fig. 4). Most  
247 notably, invasion speed variance increased approaching the threshold of zero population growth  
248 rates in both scenarios, though most dramatically in the second (bottom row of Fig. 4), and  
249 declined as the proportion of good years increased. Variance in invasion speed also increased  
250 as environmental correlations shifted from strongly negative to strongly positive. Hence, the  
251 combinations of environmental states that yielded the fastest invasion speeds also showed the  
252 highest variance in invasion speed.

253 Comparing between scenarios, the scenario with a higher average growth rate between  
254 years (top row of Fig. 4) exhibited a lower threshold for positive growth rates with respect to  
255 the frequency of good years and overall lower variance in invasion speeds, as expected. Since  
256 positive invasion speeds increased roughly linearly with the proportion of good years, a necessary  
257 outcome was that each increment of change in the proportion of good years led to a greater  
258 proportional increase in invasion speed in the “worse” scenario (bottom row of Fig. 4) than  
259 the scenario in which average growth rate across years was higher (top row of Fig. 4). In the  
260 context of real systems, this means that we might expect to observe particularly steep increases  
261 in invasion speed in response to increased frequency of good years in regions where bad years  
262 are particularly bad. In particular, changes in the frequency of El Niño years or in the temporal  
263 correlation between El Niño events, could substantially affect rates of spread of *Calathea*.

## 264 Discussion

265 How environmental variation influences population dynamics and biodiversity is a central  
266 question in ecology (Andrewartha and Birch 1954; May 1975; Tuljapurkar 1982; Chesson 2000;  
267 Holyoak et al. 2005). In our era of increasing climate variability and accelerating global trans-  
268 port of species at rates and distances far beyond their innate capacity (Vitousek et al. 1997),  
269 this question is not only academic but also directly relevant to wildlife management and the  
270 maintenance of regional biodiversity. The ability to forecast and mitigate impacts of success-  
271 ful invaders, and changes in the distribution of native species, relies on an enhanced under-  
272 standing of the potential impacts of environmental variability on population growth rates and  
273 invasion speeds (Neubert et al. 2000; Collingham and Huntley 2000). By extending a class of  
274 stage-structured integrodifference equation models to variable environments, we developed and

275 applied a methodology for examining how environmental variability and temporal correlations  
276 impact stochastic growth rates, invasion speeds, and uncertainty in invasion speed predictions.

277 For structured populations in fluctuating environments, our analysis reveals that invasion  
278 speeds are approximately normally distributed and identifies data requirements for estimating  
279 the mean and variance of invasion speeds. As shown by Neubert et al. (2000) for unstructured  
280 populations in serially uncorrelated environments, we found that variance in invasion speeds de-  
281 cay in time. Hence, the greatest uncertainty in predicting the spatial extent of an invader occurs  
282 in the earliest stages of spatial spread. The data requirements for quantifying this uncertainty  
283 are two-fold. To capture the effects of environmental fluctuations on demography, estimates of  
284 survivorship, fecundity, and transition rates between different stages are needed for the range of  
285 environmental conditions most likely to be encountered by the population (Caswell 2001; Boyce  
286 et al. 2006). Our methods also require estimates for the dispersal kernel associated with each  
287 demographic transition under an appropriate range of environmental conditions. While getting  
288 such estimates is challenging, our methods can help focus empirical efforts by identifying which  
289 stage-specific demographic rates have the largest effect on the mean and variance of the invasion  
290 speed. More generally, they can be used as an exploratory tool to identify key features of how  
291 environmental variability and stage-structure interact to determine invasion speeds.

292 Our examples illustrate several important general effects of environmental variability on  
293 invasion speeds, and point to the ways in which the outcomes of environmental-demographic  
294 interactions might vary between species. The results of our two-stage example with fluctuating  
295 fecundities showed growth rates and invasion speeds declining as the magnitude of variance  
296 in vital rates increased. This result is consistent with earlier work showing that increases in  
297 the magnitude of environmental (e.g. climate) variability tend to reduce population growth  
298 rates (Lewontin and Cohen 1969). Theory and empirical findings predict that the magnitude of  
299 these effects on population growth will depend on a species' life history: short-lived species are  
300 more negatively affected by increased variation in vital rates than longer-lived species (Chesson  
301 1985; Morris et al. 2008). Although not investigated here, it seems reasonable to conjecture that  
302 these life history traits will have similar effects on invasion speeds.

303 While increasing environmental variability reduces growth and invasion speed, correlations  
304 between environmental states can have a substantial impact on the direction and variance in  
305 growth and wave speed. Our analysis of a general unstructured model and two structured models

306 shows that positive temporal correlations between environmental states (reddened spectrum in  
307 figures) created greater variability in growth rates and invasion speeds, even at low levels of envi-  
308 ronmental noise. This finding is consistent previous work, which shows potentially strong effects  
309 of positive temporal correlations in vital rates on variance in population growth (Tuljapurkar  
310 and Orzack 1980; Tuljapurkar 1982; Runge and Moen 1998). In contrast to the consistent effect  
311 of correlations on variance, the direction of effects on expected growth rates and invasion speeds  
312 differed between examples. The general unstructured model shows no effect, which suggests  
313 that demographic structure allows for effects to go in either direction. Positive environmental  
314 correlations yielded negative effects on both stochastic growth rates and invasion speeds in the  
315 two-stage model, but positive effects in the empirically based *Calathea* model. Similarly, the  
316 direction of effects of correlations have been shown to vary in a life history context as well: serial  
317 correlations can have strongly positive or negative effects on fitness, depending on the structure  
318 of life history and the nature of within-year (among reproductive classes) and between-year  
319 correlations in fertilities in response to environmental variation (Tuljapurkar et al. 2009).

320 We also found that the magnitude of effect of environmental correlations differed between  
321 examples. In the *Calathea* example, the effect of correlations was small relative to the impor-  
322 tance of the overall proportion of years with positive growth rates, and was more limited than  
323 in the two-stage model. Limited effects of temporal environmental correlations on long-term  
324 stochastic growth rates have been observed in other empirical studies (Silva et al. 1991), and  
325 theoretical studies have found relatively minor effects of temporal correlation in vital rates on  
326 stochastic growth rates (Tuljapurkar 1982; Fieberg and Ellner 2001). However, the effects of  
327 temporal autocorrelation can be great under some circumstances, depending on life history and  
328 how well vital rates “remember” the past (Tuljapurkar and Haridas 2006). Populations with  
329 weak demographic damping (strong transient effects) tend to accumulate greater variability  
330 over time than those with strong damping, and these effects vary with the magnitude of serial  
331 correlation (Tuljapurkar and Haridas 2006).

332 Although the *Calathea* example showed relatively small effects of correlations overall, cor-  
333 relations still had the potential to substantially influence growth rates and invasion speed under  
334 some conditions, especially for populations near the threshold of positive and negative growth  
335 rates. In these threshold cases, strongly positive correlations resulted in the fastest invasion  
336 speeds, and also generally the greatest variance in those speeds. This suggests that, on the  
337 ground, changes in environmental correlations could lead to sudden or episodic changes in inva-

338 sion rates for species experiencing threshold growth conditions. These kinds of dynamics might  
339 contribute to common observations of a lag between establishment and spread of most introduced  
340 species, even those that eventually become invasive, alongside other factors such as adaptation  
341 and hybridization with native species (Ellstrand and Schierenbeck 2000; Mack et al. 2000; Sakai  
342 et al. 2001). Among native species responding to climate change, these results suggest that  
343 we might expect to observe great variation in rates of range expansion, since populations at  
344 the edge of species ranges are most likely to exist close to the threshold between positive and  
345 negative population growth. In either case, the increased variability in stochastic growth rates  
346 and invasion speed around threshold conditions will make biological expansions and invasions  
347 harder to forecast. For species characterized by substantial interannual variation and volatility  
348 in vital rates, accurately forecasting rates of spread may be particularly challenging.

349 Several factors must be taken into careful account in applying integrodifference equation  
350 models to invasions on real landscapes. For one, it is critical to understand the basic nature  
351 of relevant environmental factors and whether a given form of disturbance imposes different  
352 consequences when rare than it does when chronic (Tuljapurkar and Haridas 2006). For example,  
353 Tuljapurkar and Haridas point out that an increase in the frequency of hurricanes may weaken  
354 autocorrelation by preventing successional change, thereby effectively reducing demographic  
355 variability and the effects of autocorrelation over time despite the outward perception of dramatic  
356 environmental variation. Similarly, single years or short-term strings of conditions (e.g., warm  
357 years) may boost demographic rates for a given species, while extended autocorrelated series  
358 would lead to more substantial ecological changes (e.g., aridification) that negatively impact  
359 habitat suitability and represent non-Markovian dynamics. The models we present are applicable  
360 to increasing climatic variability but not to sustained directional changes over time. In the  
361 context of climate change, these models are likely sufficient to describe many regions of the globe,  
362 where increasing climate variability is expected to obscure the effects of concurrent directional  
363 trends over much of the next century (IPCC 2007), but not appropriate for regions where  
364 trending changes in temperature are more acute.

365 Despite these limitations, our methods provide a first step in estimating invasion speeds  
366 for populations experiencing stage-specific temporal variation in survivorship, transition rates  
367 between stages, fecundity, and dispersal. Using these methods to investigate the effects of  
368 temporal correlations on rates of invasion across a wider range of life histories and dispersal  
369 types will be an important next step.



REFERENCES

370

371 H.G. Andrewartha and L.C. Birch. *The distribution and abundance of animals*. University of  
372 Chicago Press, 1954.

373 L. Arnold, V. M. Gundlach, and L. Demetrius. Evolutionary formalism for products of positive  
374 random matrices. *Annals of Applied Probability*, 4:859–901, 1994.

375 M. S. Boyce, C. V. Haridas, C. T. Lee, and the NCEAS Stochastic Demography Working Group.  
376 Demography in an increasingly variable world. *Trends in Ecology & Evolution*, 21(3):141  
377 – 148, 2006.

378 D. Schemske C. Horvitz and H. Caswell. The importance of life history stages to population  
379 growth: prospective and retrospective analyses. In S. Tuljapurkar and H. Caswell, editors,  
380 *Structured population models in marine, terrestrial and freshwater systems*, pages 247–  
381 272, New York, New York, USA, 1997. Chapman and Hall.

382 H. Caswell. *Matrix Population Models*. Sinauer, Sunderland, Massachusetts, 2001.

383 H. Caswell, R. Lensink, and M. G. Neubert. Demography and dispersal: Life table response  
384 experiments for invasion speed. *Ecology*, 84(8):1968–1978, 2003.

385 P.L. Chesson. General theory of competitive coexistence in spatially-varying environments.  
386 *Theoretical Population Biology*, 58:211–237, 2000.

387 P.L. Chesson. Coexistence of competitors in spatially and temporally varying environments:  
388 a look at the combined effects of different sorts of variability. *Theoretical Population*  
389 *Biology*, 28:263–287, 1985.

390 Y.C. Collingham and B. Huntley. Impacts of habitat fragmentation and patch size upon migra-  
391 tion rates. *Ecological Applications*, 10(1):131–144, 2000.

392 R. Durrett. *Probability: Theory and examples*. Duxbury Press, Belmont, CA, 1996.

393 D.R. Easterling, G.A. Meehl, C. Parmesan, S.A. Changnon, T.R. Karl, and L.O. Mearns. Cli-  
394 mate extremes: observations, modeling, and impacts. *Science*, 289:2068, 2000.

- 395 N. C. Ellstrand and K. A. Schierenbeck. Hybridization as a stimulus for the evolution of inva-  
396 siveness in plants? *Proceedings of the National Academy of Sciences of the United States*  
397 *of America*, 97:7043–7050, 2000.
- 398 C. S. Elton. *The Ecology of Invasion by Animals and Plants*. Methuen, 1958.
- 399 J. Fieberg and S.P. Ellner. Stochastic matrix models for conservation and management: a  
400 comparative review of methods. *Ecology Letters*, 4(3):244–266, 2001.
- 401 R.A. Fisher. The wave of advance of advantageous genes. *Ann. Eugenics*, 7:269, 1937.
- 402 C. V. Haridas and S. Tuljapurkar. Elasticities in variable environments: properties and impli-  
403 cations. *The American Naturalist*, 166:481–495, 2005.
- 404 R. Hengeveld. Small-step invasion research. *Trends in Ecology & Evolution*, 9:339–342, 1994.
- 405 C.C. Heyde and J.E. Cohen. Confidence intervals for demographic projections based on products  
406 of random matrices. *Theoretical Population Biology*, 27(2):120–153, 1985.
- 407 M. Holyoak, M. A. Leibold, and R. D. Holt, editors. *Metacommunities: Spatial dynamics and*  
408 *ecological communities*. University of Chicago Press, 2005.
- 409 C. C. Horvitz and A. J. Beattie. Ant dispersal of *Calathea* (Marantaceae) seeds by carnivorous  
410 ponerines (Formicidae) in a tropical rain forest. *American Journal of Botany*, 67:321–326,  
411 1980.
- 412 C. C. Horvitz and D. W. Schemske. Seed dispersal of a neotropical myrmecochore: variation in  
413 removal rates and dispersal distance. *Biotropica*, 18:319–323, 1986.
- 414 C. C. Horvitz and D. W. Schemske. Spatiotemporal variation in demographic transitions of a  
415 tropical understory herb: projection matrix analysis. *Ecological Monographs*, 65:155–192,  
416 1995.
- 417 H. Jacquemyn, R. Brys, and M. G. Neubert. Fire increases invasive spread of *molinia caerulea*  
418 mainly through changes in demographic parameters. *Ecological Applications*, 15(6):2097–  
419 2108, 2005.

- 420 E. Jongejans, K. Shea, O. Skarpaas, D. Kelly, A.W. Sheppard, and T.L. Woodburn. Dispersal  
421 and demography contributions to population spread of *Carduus nutans* in its native and  
422 invaded ranges. *Journal of Ecology*, 96:687–697, 2008.
- 423 C.S. Kolar and D.M. Lodge. Progress in invasion biology: predicting invaders. *Trends in Ecology*  
424 & *Evolution*, 16(4):199–204, 2001.
- 425 M. Kot, M. A. Lewis, and P. van den Driessche. Dispersal data and the spread of invading  
426 organisms. *Ecology*, 77:2027–2042, 1996.
- 427 R. C. Lewontin and D. Cohen. On population growth in a randomly varying environment.  
428 *Proceedings of the National Academy of Sciences of the USA*, 62:1056–1060, 1969.
- 429 R.N. Mack, D. Simberloff, W. Mark Lonsdale, H. Evans, M. Clout, and F.A. Bazzaz. Biotic  
430 invasions: causes, epidemiology, global consequences, and control. *Ecological applications*,  
431 10(3):689–710, 2000.
- 432 R. M. May. *Stability and Complexity in Model Ecosystems, 2nd edn.* Princeton University Press,  
433 Princeton, 1975.
- 434 W.F. Morris, C.A. Pfister, S. Tuljapurkar, C.V. Haridas, C.L. Boggs, M.S. Boyce, Emilio M.  
435 Bruna, Don R. Church, Tim Coulson, D.F. Doak, S. Forsyth, J. Gaillard, C.C. Horvitz,  
436 S. Kalisz, B.E. Kendall, T.M. Knight, C.T. Lee, and E.S. Menges. Longevity can buffer  
437 plant and animal populations against changing climatic variability. *Ecology*, 89:19–25,  
438 2008.
- 439 M. G. Neubert and H. Caswell. Demography and dispersal: Calculation and sensitivity analysis  
440 of invasion speed for structured populations. *Ecology*, 81:1613–1628, 2000.
- 441 M. G. Neubert, M. Kot, and M. A. Lewis. Invasion speeds in fluctuating environments. *Pro-*  
442 *ceedings of Royal Society of London B*, 267:1603–1610, 2000.
- 443 M.C. Runge and A.N. Moen. A modified model for projecting age-structured populations in  
444 random environments. *Mathematical Biosciences*, 150(1):21–41, 1998.
- 445 A. K. Sakai, F. W. Allendorf, J. S. Holt, D. M. Lodge, J. Molofsky, K. A. With, S. Baughman,  
446 R. J. Cabin, J. E. Cohen, N. C. Ellstrand, D. E. McCauley, P. O’Neil, I. M. Parker, J. N.

- 447 Thompson, and S. G. Weller. The population biology of invasive species. *Annual Review*  
448 *of Ecology and Systematics*, 32:305–332, 2001.
- 449 J. F. Silva, J. Raventos, H. Caswell, and M. C. Trevisan. Population responses to fire in a  
450 tropical savanna grass, andropogon semiberbis: a matrix model approach. *Journal of*  
451 *Ecology*, 79:345–355, 1991.
- 452 C. Tebaldi, K. Hayhoe, J.M. Arblaster, and G.A. Meehl. Going to the extremes. *Climatic*  
453 *Change*, 79(3):185–211, 2006.
- 454 S. Tuljapurkar. Population dynamics in variable environments. II. Correlated environments,  
455 sensitivity analysis and dynamics. *Theoretical Population Biology*, 21:114–140, 1982.
- 456 S. Tuljapurkar. *Population Dynamics in Variable Environments*. Springer-Verlag, New York,  
457 1990.
- 458 S. Tuljapurkar and C. V. Haridas. Temporal autocorrelation and stochastic population growth.  
459 *Ecology Letters*, 9:327–337, 2006.
- 460 S. Tuljapurkar, C.C. Horvitz, and J.B. Pascarella. The many growth rates and elasticities of  
461 populations in random environments. *The American Naturalist*, 162(4):489–502, 2003.
- 462 S. Tuljapurkar, J.M. Gaillard, and T. Coulson. From stochastic environments to life histories  
463 and back. *Philosophical Transactions of the Royal Society Part B*, 364:1499–1509, 2009.
- 464 S.D. Tuljapurkar and S.H. Orzack. Population dynamics in variable environments I. Long-run  
465 growth rates and extinction. *Theoretical Population Biology*, 18(3):314–342, 1980.
- 466 P.M. Vitousek, H.A. Mooney, J. Lubchenco, and J.M. Melillo. Human domination of Earth's  
467 ecosystems. *Science*, 277:494–499, 1997.
- 468 H.F. Weinberger. Long-time behavior of a class of biological models. *SIAM Journal on Mathe-*  
469 *matical Analysis*, 13:353, 1982.

470

### A. Mathematical Details

471

We begin by considering solutions to the linear equation

$$\mathbf{n}_{t+1}(x) = \int_{-\infty}^{\infty} [\mathbf{K}_t(x-y) \circ \mathbf{A}_t] \mathbf{n}_t(y) dy \quad (\text{A.1})$$

472

Consider  $\mathbf{n}_0(x) = \mathbf{u}e^{-sx}$  with  $\mathbf{u} > 0$ . We claim that

$$\mathbf{n}_t(x) = \mathbf{H}_{t-1}(s) \dots \mathbf{H}_0(s) \mathbf{u}e^{-sx} \quad (\text{A.2})$$

473

Indeed, we show this inductively. For  $t = 1$ ,

$$\begin{aligned} \mathbf{n}_1(x) &= \int_{-\infty}^{\infty} [\mathbf{K}_0(y-x) \circ \mathbf{A}_0] \mathbf{u}e^{-sy} dy \\ &= \int_{-\infty}^{\infty} [\mathbf{K}_0(z) \circ \mathbf{A}_0] e^{-sz} dz \mathbf{u}e^{-sx} \quad \text{where } z = y - x \\ &= \mathbf{H}_0(s) \mathbf{u}e^{-sx} \end{aligned}$$

474

Next we assume that (A.2) holds for  $t - 1$ . Then

$$\begin{aligned} \mathbf{n}_{t+1}(x) &= \int_{-\infty}^{\infty} [\mathbf{K}_t(y-x) \circ \mathbf{A}_t] \mathbf{n}_t(y) dy \\ &= \int_{-\infty}^{\infty} [\mathbf{K}_t(y-x) \circ \mathbf{A}_t] \mathbf{H}_{t-1}(s) \dots \mathbf{H}_0(s) \mathbf{u}e^{-sy} dy \\ &= \int_{-\infty}^{\infty} [\mathbf{K}_t(z) \circ \mathbf{A}_t] e^{-sz} dz \mathbf{H}_{t-1}(s) \dots \mathbf{H}_0(s) \mathbf{u}e^{-sx} \quad \text{where } z = y - x \\ &= \mathbf{H}_t(s) \mathbf{H}_{t-1}(s) \dots \mathbf{H}_0(s) \mathbf{u}e^{-sx} \end{aligned}$$

475

which completes the inductive proof of (A.2).

476

Let  $X_t(s)$  be such that  $\langle \mathbf{n}_t(X_t(s)), \mathbf{w} \rangle = n_c$ . Then  $\langle \mathbf{n}_0(X_0(s)), \mathbf{w} \rangle = \langle \mathbf{n}_t(X_t(s)), \mathbf{w} \rangle$  and

477

(A.2) imply that

$$\langle \mathbf{u}e^{-sX_0(s)}, \mathbf{w} \rangle = \langle \mathbf{H}_{t-1}(s) \dots \mathbf{H}_0(s) \mathbf{u}e^{-sX_t(s)}, \mathbf{w} \rangle$$

478

equivalently

$$X_t(s) - X_0(s) = \frac{1}{s} \ln \frac{\langle \mathbf{H}_{t-1}(s) \dots \mathbf{H}_0(s) \mathbf{u}, \mathbf{w} \rangle}{\langle \mathbf{u}, \mathbf{w} \rangle}$$

479

Equation (4) implies that  $\lim_{t \rightarrow \infty} \frac{X_t(s) - X_0(s)}{t} = \frac{\gamma(s)}{s}$  with probability one.

480 Now consider an initial condition  $\mathbf{n}_0(x)$  with compact support for the non-linear model (3).  
 481 Given any  $s > 0$ , choose  $\mathbf{u} > 0$  such that  $\mathbf{n}_0(x) \leq \mathbf{u}e^{-sx}$ . Our assumption that  $\mathbf{B}_t(\mathbf{n}) \leq \mathbf{A}_t$   
 482 implies that

$$\mathbf{n}_t(x) \leq \mathbf{H}_{t-1}(s) \dots \mathbf{H}_0(s) \mathbf{u} e^{-sx}$$

483 Thus  $X_t \leq X_t(s)$  where  $X_t$  is such that  $\langle \mathbf{n}_t(X_t), \mathbf{w} \rangle = n_c$ . Hence, with probability one,

$$\limsup_{t \rightarrow \infty} \frac{X_t - x_0}{t} \leq \gamma(s)/s$$

484 Since this holds for any  $0 < s < \hat{s}$ , it follows that

$$\limsup_{t \rightarrow \infty} \frac{X_t - x_0}{t} \leq \min_{0 < s < \hat{s}} \gamma(s)/s$$

485 with probability one. The Linearization Conjecture implies that

$$\lim_{t \rightarrow \infty} \frac{X_t - x_0}{t} = \min_{0 < s < \hat{s}} \gamma(s)/s =: c^*$$

## 486 B. Log-normal approximation

487 Let  $s^*$  be such that  $\gamma(s^*)/s^* = c^*$ . Assume that  $\mathbf{H}_1(s^*), \mathbf{H}_2(s^*), \dots$  are rapidly mixing (see,  
 488 e.g., Tuljapurkar (1990); Heyde and Cohen (1985) for definitions). Then Theorem 1 in (Heyde  
 489 and Cohen 1985) implies that there exists  $\sigma \geq 0$  such that

$$\frac{\ln \langle \mathbf{H}_{t-1}(s^*) \dots \mathbf{H}_0(s^*) \mathbf{u}, \mathbf{w} \rangle - c^* s^* t}{\sqrt{t\sigma}}$$

490 converges in distribution to a standard normal as  $t \rightarrow \infty$ .